Expression and modulation of an invertebrate presynaptic calcium channel alpha 1 subunit homolog

Spafford, J.D.; Chen, L.N.; Zeng, Z.P.; Smit, A.B.; Zamponi, G.W.

published in
Journal of Biological Chemistry
2003

DOI (link to publisher)
10.1074/jbc.M302212200

document version
Publisher's PDF, also known as Version of record

THE JOURNAL OF BIOLOGICAL CHEMISTRY
Vol. 278, No. 23, Issue of June 6, pp. 21178–21187, 2003
Printed in U.S.A.

Expression and Modulation of an Invertebrate Presynaptic Calcium Channel α_1 Subunit Homolog*

Received for publication, March 3, 2003, and in revised form, April 1, 2003
Published, JBC Papers in Press, April 2, 2003, DOI 10.1074/jbc.M302212200

J. David Spafford‡§¶, Lina Chen‡, Zhong-Ping Feng‡‖, August B. Smit§, and Gerald W. Zamponi‡**

From the ‡Department of Physiology and Biophysics, Cellular and Molecular Neurobiology Research Group, University of Calgary, Calgary, T2N 4N1, Canada and §Department of Molecular and Cellular Neurobiology, Research Institute Neurosciences, Vrije Universiteit, 1081 HV Amsterdam, The Netherlands

Here we report the first assessment of the expression and modulation of an invertebrate α_1 subunit homolog of mammalian presynaptic Ca_v2 calcium channels (N-type and P/Q-type) in mammalian cells. Our data show that molluscan channel (LCa_v2a) isolated from *Lymnaea stagnalis* is effectively membrane-targeted and electrophysiologically recordable in tsA-201 cells only when the first 44 amino acids of LCa_v2a are substituted for the corresponding region of rat $Ca_v2.1$. When coexpressed with rat accessory subunits, the biophysical properties of LCa_v2a-5′rbA resemble those of mammalian N-type calcium channels with respect to activation and inactivation, lack of pronounced calcium dependent inactivation, preferential permeation of barium ions, and cadmium block. Consistent with reports of native *Lymnaea* calcium currents, the LCa_v2a-5′rbA channel is insensitive to micromolar concentrations of ω-conotoxin GVIA and is not affected by nifedipine, thus confirming that it is not of the L-type. Interestingly, the LCa_v2a-5′rbA channel is almost completely and irreversibly inhibited by guanosine 5′-3-*O*-(thio)triphosphate but not regulated by syntaxin1, suggesting that invertebrate presynaptic calcium channels are differently modulated from their vertebrate counterparts.

Calcium entry through voltage-gated calcium channels mediates a plethora of cytoplasmic responses, including the activation of enzymes, the initiation of gene transcription, neurite outgrowth and neurotransmitter release (1–3). Based on their functional and pharmacological profiles, voltage-gated calcium channels have been classified into T-, N-, L-, P/Q-, and R-types, each with unique physiological roles (1). With the exception of the T-types, voltage-gated calcium channels are heteromultimers comprised of a principal α_1 subunit that defines the calcium channel subtype plus the accessory β (4), α_2-δ (5), and possibly γ (6) subunits which modulate the functional and pharmacological properties of the α_1 subunit (1, 7). Molecular cloning has identified 4 genes, each encoding β and α_2-δ subunits, 8 genes encoding γ subunits, and 10 genes representing different types of calcium channel α_1 subunits (1). The various α_1 subunits fall into three distinct classes. The Ca_v1 class encodes L-type calcium channels, $Ca_v2.1$, $Ca_v2.2$, and $Ca_v2.3$, respectively, represent P/Q-type, N-type, and R-type channels, and Ca_v3 encodes the family of T-type calcium channels (1).

$Ca_v2.1$ (P/Q-type) and $Ca_v2.2$ (N-type) channels are densely localized at presynaptic zones of vertebrate neurons (8–10) where they are physically coupled to proteins of the synaptic vesicle release proteins such as syntaxin1, SNAP25, and synaptotagmin (1, 2, 7, 11). This possibly serves to optimize the efficiency of synaptic transmission and as a negative feedback mechanism allowing the regulation of calcium channel activity during various steps of exocytosis (7, 12). Mammalian N-type and P/Q-type calcium channels are differentially inhibited upon activation of G protein-coupled receptors (7, 13–15). This effect is mediated by G protein $\beta\gamma$ subunits and may serve to fine-tune synaptic activity.

Invertebrate species do not appear to contain the same structural diversity of vertebrate calcium channel genes in their genomes and, with one possible exception (16), possess only single homologs of the three major calcium channel families, Ca_v1, Ca_v2, and Ca_v3 (12, 17). Invertebrate Ca_v2 representatives are considered functional as well as structural correlates of both mammalian N- ($Ca_v2.2$) and P/Q-type ($Ca_v2.1$) calcium channels (12, 17). Ca_v2 homologs from *Drosophila* (DmCa1A/cac) (18, 19), *Caenorhabditis elegans* (unc-2) (20), and more recently, the freshwater mollusk *Lymnaea stagnalis* (LCa_v2a) (21), are required for invertebrate synaptic transmission, reminiscent of the roles of N- and P/Q-type channels in mammalian synapses (3, 22). The invertebrate Ca_v2 calcium channel α_1 subunits, unlike mammalian N-type and P/Q-type calcium channels, do not display an elongated domain II-III linker region, which in mammalian synaptic channels characteristically contain interaction sites for syntaxin, SNAP-25, and synaptotagmin (19, 21). However, although full-length sequences of invertebrate presynaptic calcium channels have been in the public domain for years, there has not been a report describing the functional expression of any of the cloned invertebrate Ca_v2 synaptic calcium channels. An exception to this is a single report of expression of a squid Ca_v2 homolog in *Xenopus* oocytes (23), a system known to endogenously express calcium channels as well as low levels of synaptic proteins. This has precluded a detailed functional analysis of these channels and has been an obstacle to taking full advantage of invertebrate synaptic preparations to address fundamental aspects of synaptic transmission at the molecular level.

* This work was supported by an operating grant from the Canadian Institutes of Health Research (to G. W. Z.). The costs of publication of this article were defrayed in part by the payment of page charges. This article must therefore be hereby marked "*advertisement*" in accordance with 18 U.S.C. Section 1734 solely to indicate this fact.

This work is dedicated to the late Nikita Grigoriev.

¶ This author holds a postdoctoral fellowship award from the Human Frontier Science Program.

‖ This author previously held postdoctoral research fellowships from the Canadian Institutes of Health Research and the Heart and Stroke Foundation of Canada.

** This author holds a Senior Scholar Award from the Alberta Heritage Foundation for Medical Research and is a Canadian Institutes of Health Research Investigator. To whom correspondence should be addressed: Dept. of Physiology and Biophysics, University of Calgary, 3330 Hospital Dr. NW, Calgary, T2N 4N1, Canada. Tel.: 403-220-8687; Fax: 403-210-8106; E-mail: Zamponi@ucalgary.ca.

Here we report the expression and characterization of a *L. stagnalis* Ca_v2 calcium channel α_1 subunit homolog (LCa_v2a). We show that LCa_v2a channels are ineffectively targeted to the plasma membrane but that this can be overcome by the replacement of a short stretch of amino acids at the N-terminal region of LCa_v2a (44 amino acids) with its counterpart from rat $Ca_v2.1$. When coexpressed with rat β_{1b} and α_2-δ, the functional properties of the modified LCa_v2a-5′rbA calcium channel resemble in many ways those of mammalian N-type calcium channels showing similar activation and inactivation behavior, preferential permeation of barium over calcium, a lack of pronounced calcium-dependent inactivation, and complete block by cadmium ions. Consistent with what has been reported for native *Lymnaea* calcium currents in neurons (24, 25), the LCa_v2a-5′rbA channel is insensitive to micromolar concentrations of ω-conotoxin GVIA and does not have characteristics of L-type channels with regard to nifedipine sensitivity. As expected from the lack of an identifiable syntaxin binding site (21), the coexpression of the channel with *Lymnaea* syntaxin1 did not affect channel function. Interestingly, the channel was irreversibly inhibited in the presence of GTPγS[1] but not functionally affected by syntaxin1, suggesting that invertebrate calcium channels may display distinct regulation from their vertebrate counterparts.

EXPERIMENTAL PROCEDURES

Preparation of Full-length LCa_v2a and $Lsytx_{1A}$ cDNAs for Expression—Full-length cDNA homologs of *Lymnaea* Ca_v2 (LCa_v2a, GenBank™ accession number AF484082) and syntaxin1 ($Lsytx_1$, GenBank™ accession number AF484088) were constructed from fresh *Lymnaea* brain cDNA by PCR using proofreading Turbo *Pfu* (Stratagene) polymerase and primers flanking the identified start and stop codons of the open reading frame (molecular cloning of LCa_v2a and $Lsytx_1$, described in Spafford *et al.* (21)). The 2141- and 290-amino acid coding region of LCa_v2a and $Lsytx_1$ was inserted using primer-incorporated 5′ *Not*I and 3′ *Xho*I restriction sites into the polylinker of the mammalian expression vector PMT2SX. A consensus Kozak sequence was constructed in the 5′ *Not*I site immediately upstream from the start (ATG) codon, CGGCCGCCACC(ATG). When functional expression of LCa_v2a failed, the construct LCa_v2a-5′rbA was designed. For LCa_v2a-5′rbA, a silent *Mlu*I restriction site was created at arginine, position 45, and the 5′ end of rat $Ca_v2.1$ homologue (gi:203110) was inserted by PCR. This included the region of the native Kozak sequence (7 bp of the 5′-untranslated sequence) followed by the coding region of the first 77 amino acids at the N terminus of LCa_v2a, from the 5′ *Not*I site in the polylinker to the downstream *Mlu*I site.

Sequence Comparisons—*Lymnaea* genes and rat homologs were aligned using a progressive pairwise, multiple alignment in PILEUP (UNIX-based, GCG Wisconsin Package 2002, Accelrys, Madison, WI). Aligned rat genes included $Ca_v2.1$ (P/Q type) (GI:1705706), $Ca_v2.2$ (N-type) (GI:25453410), syntaxin1A (GI:417842), and syntaxin1B (GI:631888).

Preparation of LCa_v2 Polyclonal Antibody—The antigen to make the calcium channel polyclonal antibody was derived from a 15-mer peptide, KAEDNENDSEQNDND (Henk Hilkman, Netherlands Cancer Institute, Amsterdam), corresponding to amino acids 418–432 of LCa_v2a cytoplasmic I-II linker. The purity of the peptide was confirmed by matrix-assisted laser desorption ionization mass spectrometry and analytical high performance liquid chromatography. Rabbits were immunized for a 4-week period with adjuvants and antigen conjugated to the carrier protein KLH (Washington Biotechnology Inc., Baltimore, MD). IgG rabbit antiserum was tested for immunoreactivity with the antigen by spot blot.

Transient Transfection of Mammalian Cells—Human embryonic kidney tsA-201 cells were grown and transfected using standard calcium phosphate protocol (26). cDNAs transfected included a cDNA construct encoding for green fluorescent protein (Clontech), calcium channel subunits rat α_2-δ_1 and rat β_{1b}, and either LCa_v2a or LCa_v2a-5′rbA or rat $Ca_v2.2$, plus when stated, $Lsytx_{1A}$, rat syntaxin1A, or C-terminal fragment of the β-adrenergic receptor kinase (β-ARKct). Cells slated for immunohistochemistry were left to incubate at 37 °C on poly-L-lysine-coated dishes, whereas those slated for electrophysiological experiments were incubated at 28 °C for 2–4 days before analysis.

LCa_v2 Immunostaining in Mammalian Cells—Mock-transfected tsA-201 cells or tsA-201 cells transfected with rat α_2-δ_1, rat β_{1b}, and either LCa_v2a or LCa_v2a-5′rbA were incubated at 37 °C for 4 days, fixed with 1% paraformaldehyde for 12 h at 4 °C, then permeabilized in 1% Nonidet-P40 (octylphenoxypolyethoxyethanol polyethyleneglycol-*p*-isooctylphenyl ether) for 1 h at room temperature. Afterward, cells were washed in TBS-BSA-Triton blocking agent (50 mM Tris, 150 mM NaCl, 1 g/liter bovine serum albumin; Sigma-Aldrich, A9647), 0.5% Triton-X100, pH 7.4, and then incubated with 1:1000 dilution, LCa_v2 anti-rabbit polyclonal antibody in TBS-BSA-Triton overnight at 4 °C. The next day cells were exposed to 10× washes in TBS-BSA-Triton and treated with a 1:500 dilution of Alexa Fluor 568 goat anti-rabbit IgG (Molecular Probes, Inc., Eugene OR) in TBS-BSA-Triton overnight at 4 °C. The next day, cells were washed 10× in TBS (50 mM Tris, 150 mM NaCl, pH 7.4), wet-dried, and mounted in fluorescence anti-fading media (ProLong AntiFade, Molecular Probes). Images were visualized and analyzed on an Olympus confocal microscope.

Immunoblot Analysis of LCa_v2 and $Lsytx_1$ Protein Expression in tsA-201 Cells—Transiently transfected or untransfected tsA-201 cells incubated for 4 days at 37 °C were harvested for Western blot analysis using a standard procedure (26). Proteins were detected with primary antibodies at 1:2000 dilution, raised in rabbits against LCa_v2a or $Lsytx_1$ (ANR-002, Alomone Labs, Jerusalem, Israel). Color detection of gel blots were processed using previously described methods (21).

Functional Assessment and Analysis of LCa_v2 cDNA Expression—Calcium channel activity in transiently transfected tsA-201 cells was characterized via whole cell patch clamp using an Axopatch 200B amplifier (Axon Instruments, Union City, CA), pCLAMP 9.0 software, and previously described recording procedures and solutions (26). Data analysis was carried out using Clampfit (pClamp 9, Axon Instruments) and SigmaPlot 2000 (Jandel Scientific, SPSS Science, Chicago, IL.). Steady state inactivation curves were fit with standard Boltzmann relations $I = 1/(1 + \exp(V - V_h/S))$, where I is the normalized peak current amplitude, V is the holding potential, V_h is the half-inactivation potential, and S is a slope factor. Whole cell current voltage relations were fitted with the equation $I = G(V - E_{rev})/(1 + \exp(V_a - V)/S)$, where G is the maximum slope conductance, I is the peak current amplitude, V is the test potential, E_{rev} is the reversal potential, V_a is the half-activation potential, and S is a slope factor inversely proportional the effective gating charge. Time constants for inactivation, τ, were determined from monoexponential fits to the raw data (Fig. 3*A*). Error bars reflect S.E., and numbers in parentheses reflect numbers of experiments. Statistical analysis was carried out using Sigmastat (Jandel Scientific). Differences between mean values from each experimental group were tested using paired and unpaired Student's *t* tests and were considered significant if $p < 0.05$.

RESULTS AND DISCUSSION

The N Terminus Region of Ca_v2 Calcium Channels Regulates Membrane Trafficking—We have recently reported the effects of RNA-mediated interference knockdown of a Ca_v2 calcium channel homolog on *Lymnaea* synaptic transmission (21). Our data revealed that synaptic transmission in identified *Lymnaea* neurons was dependent on a Ca_v2 calcium channel homolog (LCa_v2a) that is capable of associating with the scaffolding proteins Mint-1 and CASK but which curiously lacks the synaptic protein interaction site common to mammalian presynaptic calcium channels (21) (see Fig. 1, *A* and *B*). To functionally characterize the LCa_v2a channels, we generated a full-length cDNA inserted in a mammalian expression vector and coexpressed the channel with rat β_{1b} and α_2-δ_1 accessory subunits and an enhanced green fluorescent protein expression marker in tsA-201 cells. Repeated attempts ($n = 24$) to record current activity via whole cell patch clamp recordings failed, consistent with the lack of any reports of expression of synaptic invertebrate calcium channels in cell lines. To determine whether our inability to record from LCa_v2a calcium channels was due to inefficient protein synthesis or membrane targeting, we generated an antibody based upon a 15-mer peptide sequence of LCa_v2a in a region of low similarity among calcium channels and, thus, a low probability of interaction with other

[1] The abbreviations used are: GTPγS, guanosine 5′-3-*O*-(thio)triphosphate; BSA, bovine serum albumin.

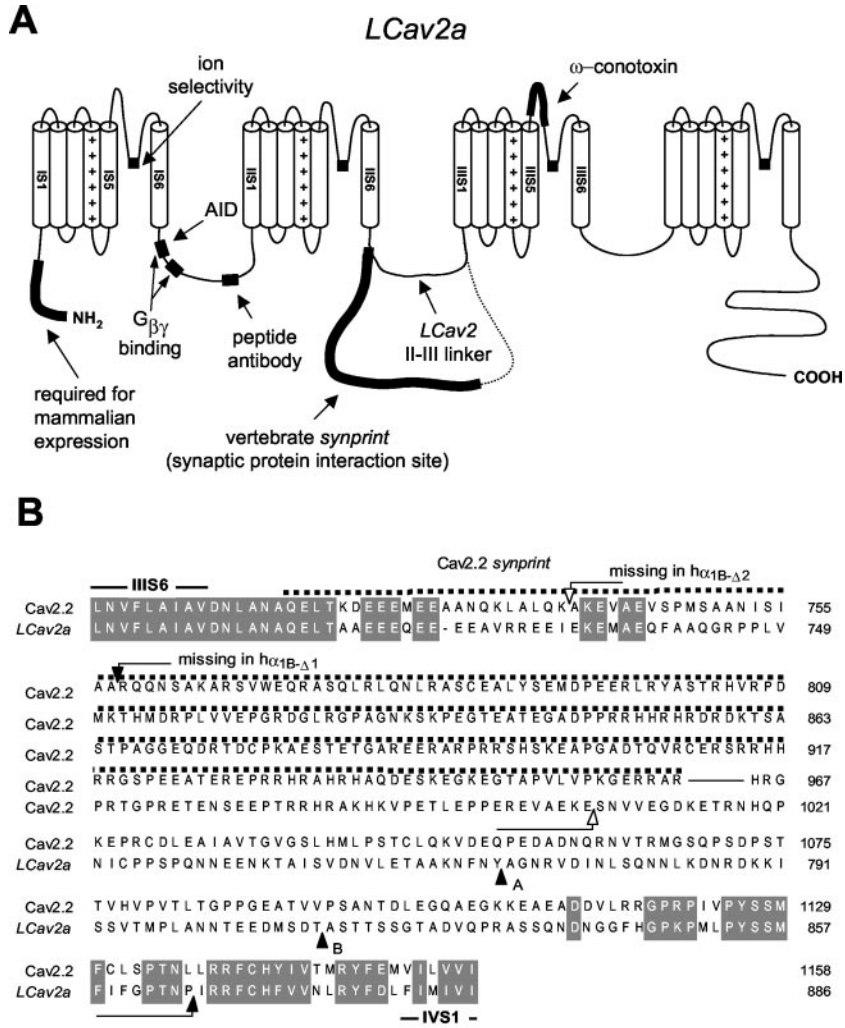

FIG. 1. *A*, schematic representation of the α_1 subunit of LCa_v2a calcium channel with highlighted regions of significance described in the text (indicated by *bold segments*). Note that the II-III linker of LCa_v2a has a dramatically shortened intracellular loop compared with rat Ca_v2 homologs. *B*, sequence alignment of the shorter II-III linker region of LCa_v2a with the equivalent region in rat $Ca_v2.2$, which is longer and contains a synaptic protein interaction (*synprint*) site common to vertebrate presynaptic calcium channels (*dotted line* above sequence). Indicated are *arrows* delimiting the homologous region in rat $Ca_v2.2$ (α_{1B}) that is absent in a human α_{1B} Δ1 and Δ2 splice variants. α_{1B} Δ2 eliminates most of the *synprint* site, and as a consequence, there is a loss of syntaxin1A binding capacity in the human II-III linker (46). (▲A) and (▲B) refer to small insertions of 4 and 13 amino acids, respectively, found within C-terminally truncated, b variant of LCa_v2.

proteins (see Fig. 1*A*). Using this antibody, we determined the expression pattern of LCa_v2a in transfected tsA-201 cells via confocal fluorescence microscopy. The antibody produced almost no background staining in mock-transfected cells (Fig. 2*A*). When cells were transfected with LCa_v2a together with appropriate ancillary subunits (Fig. 2*B*), staining could be observed in cytoplasmic compartments, but much less membrane staining was apparent, suggesting that LCa_v2a protein is synthesized but not efficiently targeted to the plasma membrane, thus accounting for the lack of barium currents in our electrophysiological analysis.

We then attempted a strategy used previously to obtain expression of a mammalian $Ca_v2.2$ calcium channel variant in *Xenopus* oocytes (27–29) by replacing part of the N-terminal region of the LCa_v2a channel (44 amino acids) with the corresponding sequence from rat $Ca_v2.1$ (creating LCa_v2a-5′rbA). As shown in Fig. 2*C*, LCa_v2a-5′rbA is detected in the plasma membrane as rings of fluorescence of differing intensities around the cell edges, apparent in approximately one-third of all transfected cells, similar to the fraction of green fluorescent protein-positive cells in typical transfections. Single bands of predicted size (~240 kDa) for LCa_v2a were detected in an immunoblot of LCa_v2a and LCa_v2a-5′rbA-transfected tsA-201 cells but not in mock-transfected cells (Fig. 2*D*). Together with the relatively low abundance of membrane staining and absence of observed barium currents in LCa_v2a-transfected cells, this indicates that the native N terminus of LCa_v2a either directly antagonizes plasma membrane trafficking in mammalian cells or that it might be missing an N-terminal domain required for efficient trafficking or stabilization of channels in mammalian cell membranes (see Fig. 2*E* for sequence alignment of the rat $Ca_v2.2$ and LCa_v2a N-terminal regions). It is interesting to note that among rat Ca_v2 channels, there is a common, almost identical 28-amino acid N-terminal sequence just upstream of where LCa_v2a differs with rat channels (see the *boxed* amino-acids, Fig. 2*E*), raising the possibility that this motif may perhaps be involved in membrane targeting. Further construction of chimeras will be needed to substantiate this possibility.

The Biophysical Properties of LCa_v2a-5′rbA Are Similar to Those of Mammalian N-type Channels—When analyzed electrophysiologically, the LCa_v2a-5′rbA channel construct resulted in robust barium currents in 46 of 82 green fluorescent protein-positive cells when transiently expressed in tsA-201 cells. This clearly contrasts with the lack of detectable expression of the wild type LCa_v2a channel. We therefore carried out a detailed analysis of biophysical properties of the LCa_v2a-5′rbA calcium channel. A shown in Fig. 3*A*, the LCa_v2a-5′rbA channel supports barium currents with moderate inactivation kinetics. As seen from the ensemble current-voltage relations (Fig. 3*B*), currents first activate at about −20 mV and peak near +20 mV. The half-activation potential determined from the fit of the IV curve was +8.5 mV, consistent with LCa_v2a-5′rbA acting as a high voltage-activated calcium channel. A similar value was obtained from fits to individual IV relations (10.8 ± 1.9 mV, n = 26). The peak of the IV curve of LCa_v2a-5′rbA is shifted about 20 mV positive to the human $Ca_v2.2$ (N-type) calcium channel (30) and about 10 mV positive to the

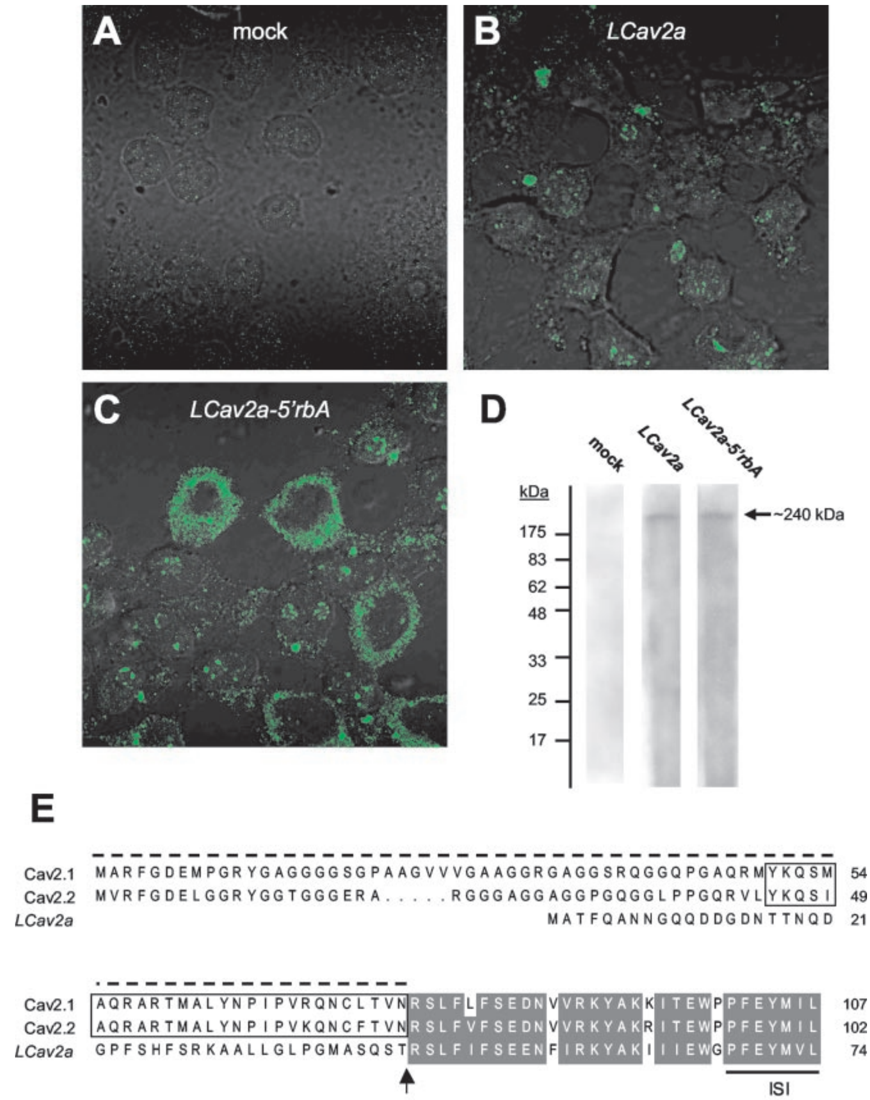

FIG. 2. *A*, *B*, and *C*, immunostained tsA-201 cells with LCa$_v$2 antibody superimposed on bright field images. tsA-201 cells were either mock-transfected (*A*) or transfected with LCa$_v$2a and rat β_{1b} + rat α_2-δ_1 (*B*) or LCa$_v$2a-5′rbA and rat β_{1b} + rat α_2-δ_1 (*C*). Note that LCa$_v$2a and LCa$_v$2a-5′rbA dramatically differ in their membrane-delimited staining. *D*, Western blot of tsA-201 protein homogenate either mock-transfected or transfected with LCa$_v$2a + rat β_{1b} + rat α_2-δ_1, or LCa$_v$2a-5′rbA + rat β_{1b} + rat α_2-δ_1 and probed with LCa$_v$2 antibody. Note that the antibody recognizes a single band of the expected ~240-kDa size in lanes containing LCa$_v$2a and LCa$_v$2a-5′rbA but not in the lane containing protein homogenate of mock-transfected cells. *E*, sequence alignment of the N-terminal regions of rat Ca$_v$2.1, rat Ca$_v$2.2, and LCa$_v$2a calcium channels. Note the large degree of sequence divergence in an alignment of the first 44 amino acids of LCa$_v$2a. The *arrow* indicates the location of the *Mlu*I site used to swap N termini of *Lymnaea* for rat Ca$_v$2.1 (*dotted line* above the sequence) to create the chimeric LCa$_v$2a-5′rbA channel. *Boxed* amino-acids represent a highly conserved sequence in vertebrate Ca$_v$2 channels.

rat Ca$_v$2.2 isoform (31) under similar experimental conditions. Steady state inactivation of the LCa$_v$2a-5′rbA channels were examined using 5-s prepulses to various holding potentials before a +20-mV test depolarization. The ensemble of the steady state inactivation curves is well described by a Boltzmann relation (Fig. 3*C*). The half-inactivation potential from the ensemble fit (−39.9 mV) and from fits to individual steady state inactivation curves (−39.6 ± 6.4 mV, n = 14) is about 10 mV more positive than that of the human Ca$_v$2.2 calcium channel (30) and about 5 mV more depolarized than that seen with rat Ca$_v$2.2 (26, 32) under these experimental conditions. As seen with mammalian calcium channels, the voltage dependence of the time constant of inactivation slightly decreases at more depolarized potentials (Fig. 3*D*).

Fig. 4*A* depicts current records obtained from the same cell in 20 mM external barium and 20 mM external calcium. As evident from these current recordings and from the current voltage relations in Fig. 4*B*, replacement of barium with calcium resulted in a dramatic reduction in peak current amplitude as seen with many other types of vertebrate mammalian high voltage-activated calcium channels. In six such paired experiments, the maximum slope conductance underwent a statistically significant reduction (from 10.5 ± 1.8 nanosiemens to 3.95 ± 0.56 nanosiemens, n = 6, $p < 0.05$) when calcium replaced barium as the external charge carrier (see the *inset* to Fig. 4*B*). This effect may be due to a reduction in single channel conductance, an effect on maximum open probability, or a combination thereof and is seen with most types of mammalian high voltage-activated calcium channels with the exception of Ca$_v$2.3 (33). These data are consistent with the observation that the selectivity filter region in the four transmembrane domains of Ca$_v$2.1 and Ca$_v$2.2 calcium channels is conserved in LCa$_v$2a (see Fig. 4*C*). In addition, the half-activation potential in this set of experiments shifted from 8.1 ± 2.5 to 26.58 ± 1.8 mV (n = 6, $p < 0.05$), as reported for a number of voltage-gated calcium channels (see Refs. 33 and 34). It is interesting to note that half-activation potential shifts of this magnitude are more typical to L-type calcium channels, with N-type and P/Q-type channels showing a smaller (~10 mV) effect (33).

We also examined the time course of inactivation in both barium and calcium. As shown in Fig. 4*C*, when the current records of Fig. 4*A* were superimposed to overlap at peak, a small degree of kinetic speeding could be observed in calcium, perhaps indicative of a small degree of calcium-sensitive inactivation. Examination of this effect at a number of different test potentials shows that calcium significantly speeds the rate of inactivation at more depolarized voltages (Fig. 4*D*). This small degree of speeding is comparable with that reported for rat P/Q-type calcium channels but much less pronounced than the calcium-dependent inactivation of L-type calcium channels. It is, however, important to note that the calcium-induced ~20-mV shift in half-activation potential could potentially re-

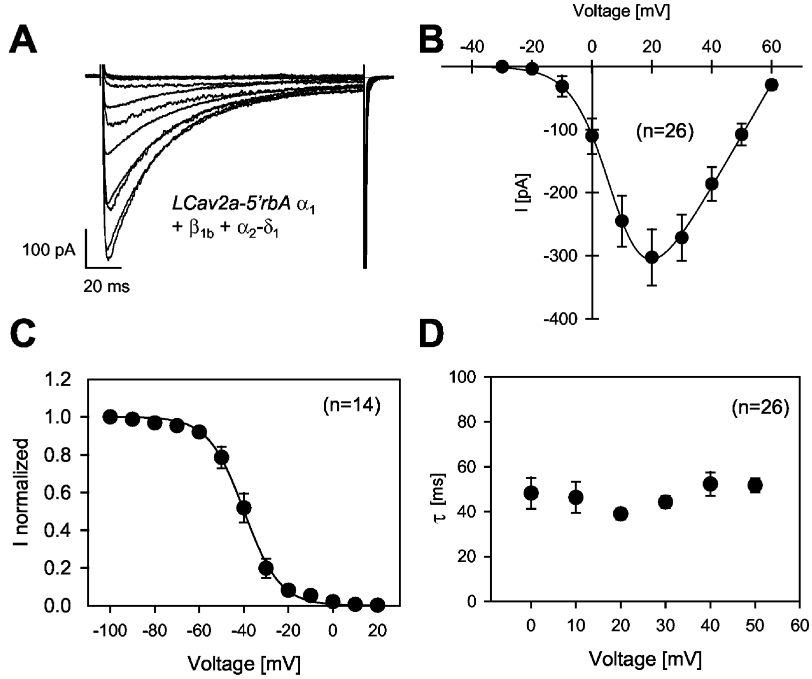

FIG. 3. *A*, family of whole cell currents recorded from the LCa$_v$2a-5′rbA calcium channel coexpressed with rat β_{1b} and α_2-δ_1 subunits. The cell was held at −100 mV and depolarized to various test potentials at 10-s intervals. *B*, ensemble of whole cell current-voltage relations from 26 different experiments. In each case, the holding potential was −100 mV. The *solid line* reflects a fit as described under "Experimental Procedures." The parameters obtained from the fit were as follows: G = 8.2 nanosiemens, S = 6.39 mV, E_{rev} = 63.3 mV, V_a = +8.5 mV. *C*, ensemble of 14 steady state inactivation curves obtained at a test potential of +20 mV. The *solid line* is a fit with the Boltzmann relation. The parameters obtained from the fit were as follows: V_h = −39.9, S = 8.04 mV. *D*, voltage dependence of the time constant of inactivation, τ, obtained at a holding potential of −100 mV. The time constants were obtained as described under "Experimental Procedures."

sult in a similar shift in the voltage dependence of the time constant for voltage-dependent inactivation, thus attributing the observed effects purely to voltage-dependent rather than calcium-dependent inactivation (*i.e.* compare the inactivation time constants in barium and calcium at +40 and +60 mV, respectively). Taken together, our data thus indicate that LCa$_v$2a-5′rbA calcium channels undergo only little if any calcium-dependent inactivation.

LCa$_v$2a-5′rbA Channels Are ω-Conotoxin GVIA-resistant—It has been shown previously that native *Lymnaea* neuronal whole cell calcium currents are insensitive to classical blockers such as ω-conotoxin GVIA and nifedipine (24, 25). Indeed, to date no selective blocker of these native currents has been identified. As shown in Fig. 5*A*, the LCa$_v$2a-5′rbA channel shows the predicted lack of nifedipine and ω-conotoxin GVIA block. At concentrations (*i.e.* 3 μM GVIA and 5 μM nifedipine) at which mammalian N-type and L-type channels would, respectively, be completely blocked (35, 36), the LCa$_v$2a-5′rbA channel showed only about a 10% reduction in peak current amplitude in response to ω-conotoxin GVIA and no detectable inhibition by nifedipine. In contrast, application of 100 μM cadmium completely abolished current activity within 10 s of application, as expected from a high voltage-activated calcium channel. The lack of conotoxin inhibition is interesting given the relatively high degree of sequence homology within the putative ω-conotoxin GVIA binding region of the Ca$_v$2.2 calcium channel domain III S5-S6 region (Fig. 5*B*, see Refs. 27 and 36). By contrast, the inhibition by cadmium ions is consistent with the sequence conservation of the narrow region of the pore (Fig. 4*E*, see Refs. 37 and 38).

LCa$_v$2a-5′rbA Is Uniquely Regulated by G Proteins—Both rat N-type and P/Q-type calcium channels are inhibited by direct interactions with G protein $\beta\gamma$ subunits (see Refs. 39–41). A hallmark of G protein inhibition of these channels is that it can be relieved after the application of a strong depolarizing prepulse (see 42, 43). Under control conditions, the application of such a prepulse resulted in a slight decrease in peak current amplitude by 13 ± 2.9% (n = 16), presumably due to a small degree of inactivation occurring during the prepulse and indicating a lack of tonic (background) G protein inhibition. To elicit a putative G protein inhibition of LCa$_v$2a-5′rbA channel activity, we added 100 μM GTPγS to the patch pipette but consistently failed to observe current activity upon cell rupture in seven experiments. In one additional experiment, however, current activity could be observed but was completely eliminated within 2 min of cell rupture and could not be recovered with application of prepulses. These data suggest the possibility that rapid dialysis of the cell with GTPγS may have resulted in an irreversible inhibition of LCa$_v$2a-5′rbA activity. To examine this possibility, the very tip of the recording pipette was filled with intracellular recording solution, and the rest of the pipette was back-filled with GTPγS-containing solution, thus allowing us to slow the dialysis of the cell with GTPγS. As shown in Fig. 6*A*, this resulted in the appearance of inward barium currents. However, unlike under control conditions, where currents remained stable over a time course of 10–15 min (not shown), channel activity decayed rapidly, presumably due to activation of G proteins in response to dialysis with GTPγS. The application of prepulses had only little effect on current amplitude, indicating that membrane depolarization was ineffective in reversing the GTPγS-mediated inhibition. For comparison, rat N-type calcium channels would under these conditions display a ~200–300% increase in peak current amplitude in response to application of the prepulse (44).

This leaves two possibilities. First, as in mammalian Ca$_v$2.2 calcium channels, G$\beta\gamma$ subunits liberated by GTPγS-induced dissociation of the heterotrimeric G protein complex could perhaps directly bind to the channel to inhibit channel opening. If so, then binding would have to be unusually tight since prepulses were ineffective in relieving the GTPγS-mediated inhibition. As seen in Fig. 6*B*, the LCa$_v$2a-5′rbA channel and the rat Ca$_v$2.2 channel share a high degree of sequence homology in the first putative G protein binding motif in the domain I-II linker (which overlaps with the calcium channel β subunit interaction site, alpha interaction domain sequence), whereas in the second putative G protein region identified in rat Ca$_v$2.1 and Ca$_v$2.2 channels (7, 15), there is little sequence similarity to the LCa$_v$2a channel. It is, thus, conceivable that this results in a more stable G protein-channel interaction that is resistant to membrane depolarization.

Alternatively, it is possible that G$\beta\gamma$ subunits might be incapable of interacting with the LCa$_v$2a-5′rbA channel. Instead,

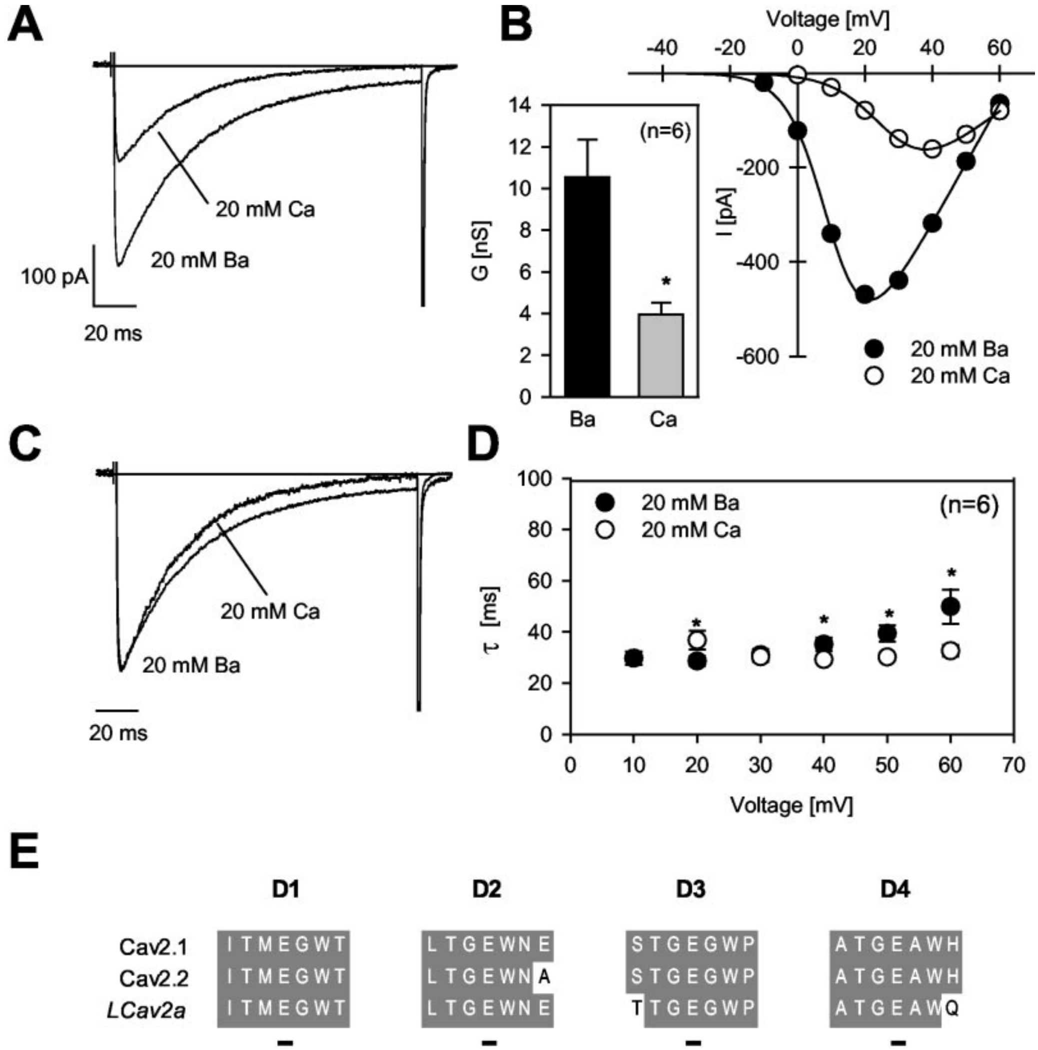

FIG. 4. *A*, whole cell recording from a LCa_v2a-5′rbA (+rat β_{1b} + rat α_2-δ_1) calcium channel in 20 mM external barium and in 20 mM external calcium at a test potential of +40 mV. The *solid line* indicates the base line. Note the reduction in peak current amplitude in external calcium. *B*, example of a typical pair of current voltage relations obtained from the same cell in either 20 mM external barium (*filled symbols*) and 20 mM external calcium (*hollow symbols*). Note the reduction in maximum slope conductance and the rightward shift in the peak of the current voltage relation in external calcium. *Inset*, comparison of the maximum slope conductance values in barium and calcium in a total of six paired experiments in form of a *bar graph*. *C*, the same whole cell currents as those shown in *panel A* but superimposed here to overlap at peak. Note the small degree of speeding of the inactivation kinetics in external calcium. *D*, time constants for inactivation obtained at various test potentials in 20 mM barium or in 20 mM calcium. In each of the six experiments included in the figure, time constants were measured under both conditions on the same cell. The *asterisks* denote statistical significance to 0.05 (paired *t* test). *E*, alignment of the putative selectivity filter contributed by conserved residues (especially conserved glutamic acid residue, *underlined*) in the pore region between segments 5 and 6 in homologous positions in the four transmembrane domains of rat $Ca_v2.1$, rat $Ca_v2.2$, and LCa_v2a calcium channels.

GTPγS might trigger an intracellular signaling cascade that could secondarily inhibit channel activity. A number of electrophysiological studies in preparations of identified molluscan neurons (including *Lymnaea*) could be consistent with the existence of such a mechanism (24). In *Helisoma*, Phe-Met-Arg-Phe-NH_2 triggers a PTX sensitive, G_o-mediated inhibition of calcium currents, which results in a depression of neurotransmitter release (45) and inhibition of growth cone motility (46). This effect could be mimicked by GTPγS and was shown to be irreversible (45, 46). Similar observations with Phe-Met-Arg-Phe-NH_2 inhibition of calcium currents have been reported for neurons of *Helix aspera*, (47), *Aplysia californica* (48), and *Lymnaea* (49). However, although there are some apparent parallels to our observations with transiently expressed LCa_v2a-5′rbA channels, it remains to be determined whether GTPγS similarly affects native *Lymnaea* synaptic calcium currents. Nonetheless, it seems clear that the regulation of transiently expressed LCa_v2a-5′rbA calcium channels appears to be fundamentally different from those of their mammalian counterparts, but additional studies will need to be conducted to pinpoint the precise signaling mechanism underlying the unique regulation of this Ca_v2 calcium channel homolog.

Syntaxin1 Regulation of the LCa_v2a-5′rbA Channel—We have shown previously that unlike the rat N-type calcium channel (1, 2, 26, 28, 32, 50), the LCa_v2a calcium channel is incapable of directly interacting with syntaxin1 (21). This is due primarily to the absence of the synaptic protein interaction site in the LCa_v2a II-III linker region (Fig. 1*B*). Hence, one would predict that the coexpression of syntaxin1, which in rat N-type calcium channels results in a pronounced hyperpolarizing shift in half-inactivation potential (28, 32, 50), should not affect LCa_v2a-5′rbA channel gating. Rather than using rat syntaxin1A or 1B, which we have characterized previously, we used *Lymnaea* syntaxin1 ($Lsytx_1$) for coexpression studies. To demonstrate expression of $Lsytx_1$ in tsA-201 cells, we first generated a Western blot of tissue homogenated from mock- and $Lsytx_1$-transfected cells probed with an antibody to rat syntaxin1 (Fig. 7*A*). We then coexpressed $Lsytx_1$ with the rat

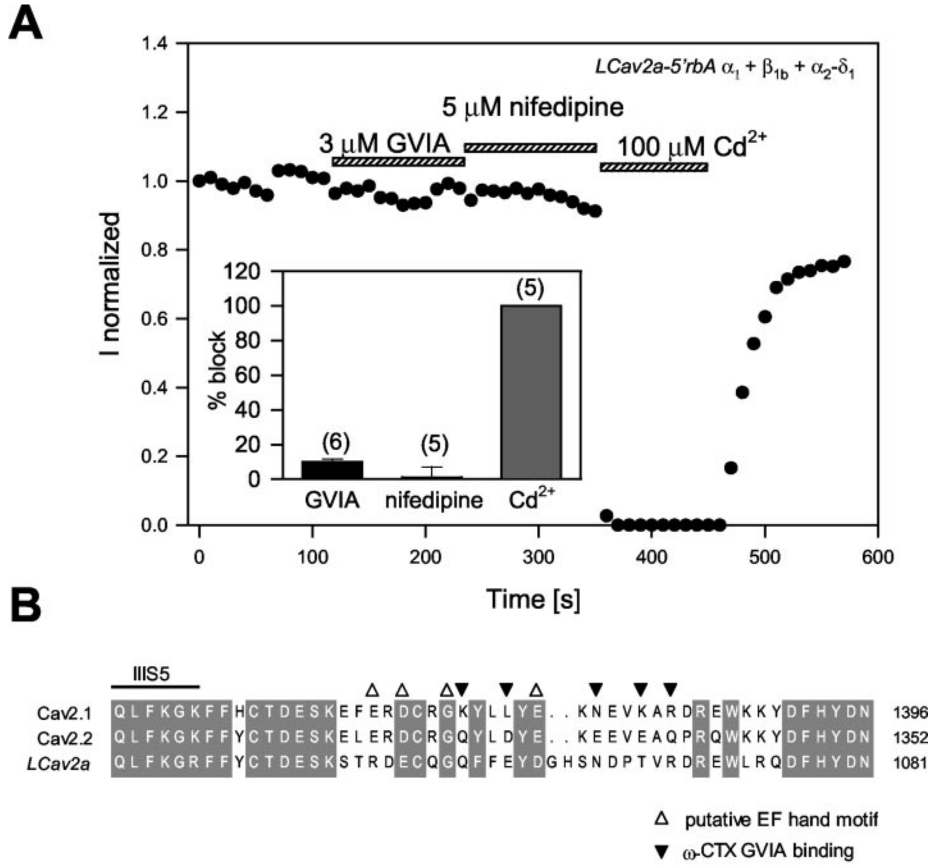

FIG. 5. *A*, representative time course of block of LCa_v2a-5′rbA calcium channels by 3 μM ω-conotoxin GVIA, 5 μM nifedipine, and 100 μM cadmium. Note that only cadmium appears to mediate significant inhibition. *Inset*, summary of the blocking effects of GVIA, nifedipine, and cadmium in the form of *bar graphs*. Cadmium always completely inhibited current activity, and hence, no *error bars* are evident. *B*, sequence alignment of the region from domain III S5 into the pore linking IIIS5 to IIIS6 of rat $Ca_v2.1$, rat $Ca_v2.2$, and the LCa_v2a calcium channels, which is considered especially critical for ω-conotoxin binding in $Ca_v2.2$ channels.

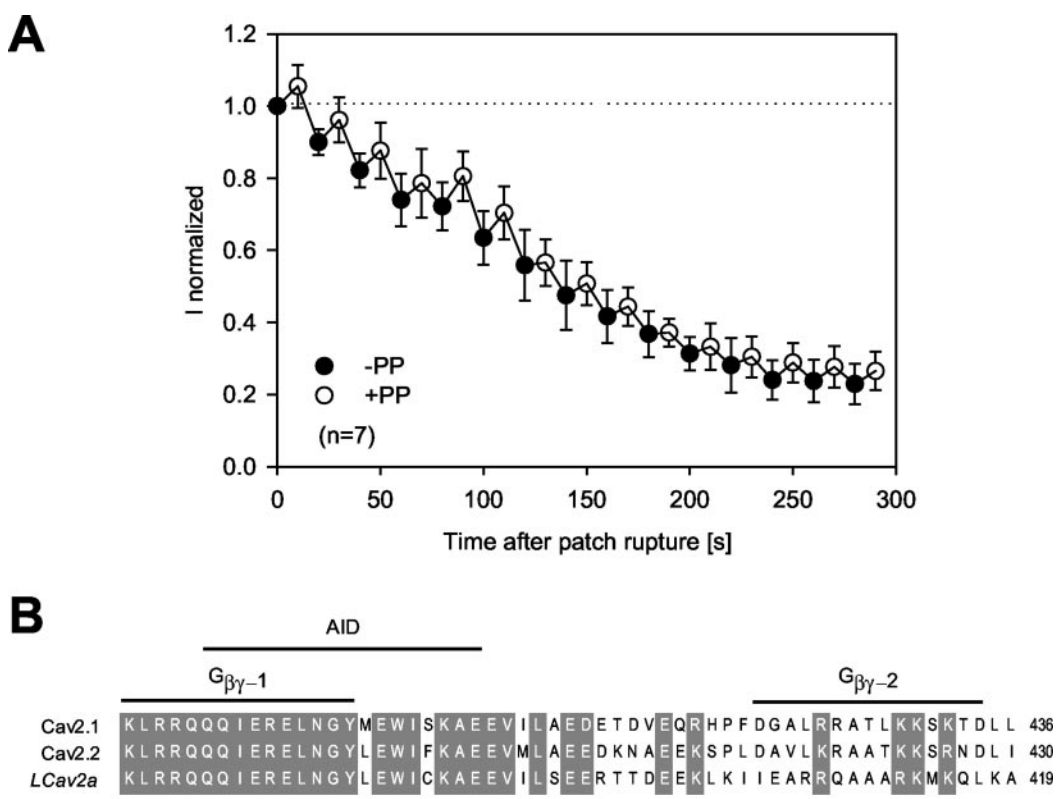

FIG. 6. *A*, time course of current amplitude in response to intracellular dialysis with 100 μM GTPγS (n = 7). Currents were elicited by stepping from −100 mV to +20 mV, and every second test pulse was preceded by a depolarizing prepulse (*PP*) to +150 mV for 50 ms (*open symbols*). For each experiment, all current amplitudes were normalized to the peak current value seen with the first test pulse. Note that current rapidly decays in response to GTPγS dialysis, but that this inhibition cannot be relieved by application of prepulses. *B*, sequence alignment of the linker region between domains I and II of rat $Ca_v2.1$, rat $Ca_v2.2$, and LCa_v2a calcium channels. Note the high degree of conservation in the first putative G$\beta\gamma$/calcium channel β subunit binding site (alpha interaction domain), which contrasts with the sequence divergence shown in the second G$\beta\gamma$ interaction site.

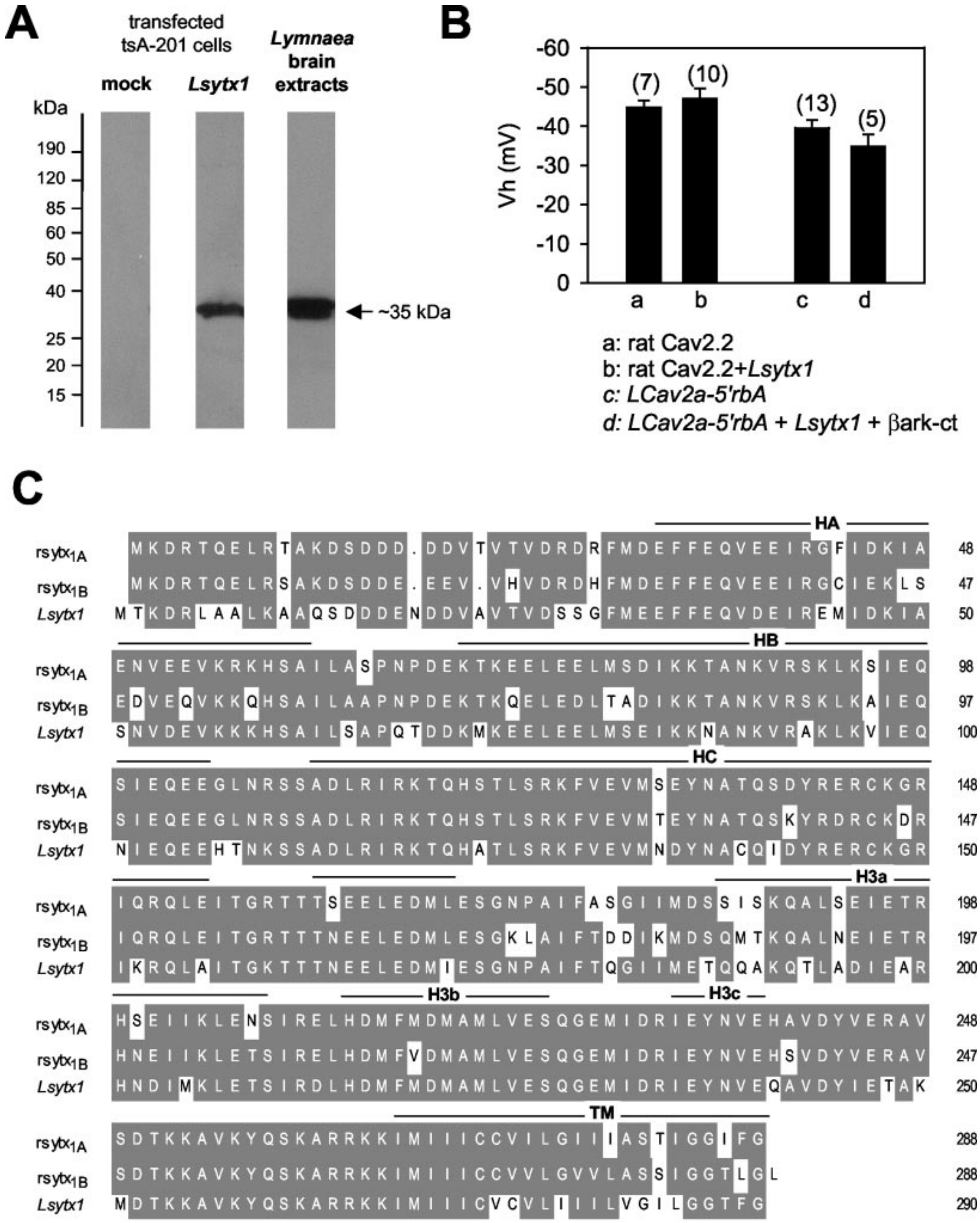

FIG. 7. *A*, Western blot stained with a syntaxin1 antibody illustrating *Lymnaea* syntaxin1 ($Lsytx_1$) expression in $Lsytx_1$-transfected tsA-201 cells (~35-kDa band) and in *Lymnaea* brain homogenate. Note the absence of signal in the control lane of the mock-transfected cells. *B*, comparison of half-inactivation potentials obtained with LCa_v2a-5′rbA or rat $Ca_v2.2$ (each coexpressed with rat β_{1b} and α_2-δ_1 subunits) with or without coexpression of $Lsytx_1$ (and as indicated, the C terminus of the β-adrenergic receptor kinase, β-ARKct, which serves as a $G\beta\gamma$ sink; see Ref. 39). Note that neither the rat N-type channel nor the LCa_v2a-5′rbA channel undergoes a negative shift half-inactivation potential. *Numbers* in *parentheses* indicate the numbers of experiments. *C*, sequence alignment of rat syntaxin1A, rat syntaxin1B and *Lymnaea* syntaxin1. Note the high degree of homology among the three syntaxin isoforms.

N-type calcium channel to determine whether $Lsytx_1$ mediated similar functional effects to those described for rat syntaxin1A, that is, a hyperpolarizing shift in the midpoint of the steady state inactivation curve, and a tonic G protein inhibition of the channel triggered by syntaxin binding to the channel, which can be assessed by application of strong depolarizing prepulse (26, 32, 50). Interestingly, unlike rat syntaxin1A and 1B, $Lsytx_1$ did not affect the position of the steady state inactivation curve of the rat N-type channel (control, $V_h = -44.8 \pm 1.7$ mV, $n = 7$; $Lsytx_1$, $V_h = -47 \pm 2.4$ mV, $n = 10$, see Fig. 7*B*) despite being able to bind to its domain II-III linker region as we showed recently (21). The lack of $Lsytx_1$ expression on rat N-type channel inactivation is, however, somewhat surprising since $Lsytx_1$ is highly homologous to both rat syntaxin1A and -1B (see Fig. 7*C*), both of which affect N-type channel gating (32). This result may, thus, provide novel clues about the syntaxin structural determinants that are required to affect N-type channel gating. In the presence of $Lsytx_1$, we did, however, detect tonic G protein inhibition of the rat N-type channel ($32 \pm 7\%$ current enhancement by the prepulse, $n = 10$, not shown), which differed significantly from background. Although this effect was not nearly as large at that described by us previously for rat syntaxin1A (~80% enhancement after the prepulse; see Ref. 32), this observation together with the Western blot shown in Fig. 7*A* suggests that $Lsytx_1$ was functionally expressed in tsA-201 cells and is active on the N-type channel.

We next examined the action of $Lsytx_1$ on the functional properties of the LCa_v2a-5′rbA calcium channel. To eliminate any syntaxin-mediated G protein inhibition that might interfere with our ability to record from the channel, we also coexpressed the C-terminal fragment of the β-adrenergic receptor kinase (β-ARKct), a known inhibitor of Gβγ-mediated signaling events (26). Under these circumstances, the half-inactivation potential of the channel was not significantly affected by the presence of $Lsytx_1$ (Fig. 7C), consistent with our previous report showing that $Lsytx_{1A}$ is incapable of binding to the channel *in vitro* (21). These data suggest that the modulation of presynaptic calcium channel gating by syntaxin1 is likely a vertebrate specialization.

Potential Limitations of Our Study—In this study, the 5′ end of rat $Ca_v2.1$ was necessary to promote the expression of this channel in mammalian cells. Without this modification, the functional description of the invertebrate channel would not have been possible, thus making use of a chimeric channel was a necessary evil. Based on previous structure function studies on mammalian calcium channels, many of the functional properties that we examined here (permeation, p loops (37, 38); voltage-dependent inactivation, I-II linker and S6 segments (51–56); calcium-sensitive inactivation, C terminus (57–60); dihydropyridine sensitivity, IIS5, IIIS6, and IVS6 segments (61, 62); conotoxin block, IIIS5-S6 region (27, 36); syntaxin regulation, II-III linker (1, 2, 7, 11, 26, 28, 32, 50)) are unlikely to be affected by the presence of the mammalian $Ca_v2.1$ N-terminal sequence. However, this may not be so with regard to G protein regulation of the channel, if it were to be mediated by a direct action of Gβγ subunits on the channel. Although the major Gβγ interaction sites on the mammalian Ca_v2 channels are found in the domain I-II linker and the C-terminal regions (15, 40, 63), the N terminus has been implicated in regulating the functional effects of G protein βγ subunits on N-type channel activity (64). Thus, whereas mammalian $Ca_v2.1$ channels are typically only weakly regulated by direct action of Gβγ (13, 39, 41), we cannot rule out the possibility that the presence of the $Ca_v2.1$ N terminus could enhance a putative direct Gβγ modulation of LCa_v2a. However, as we discussed above, in light of previous literature, it appears more likely that the GTPγS-mediated inhibition is due to an indirect regulation by one or more second messengers. Future experiments will attempt to delineate the exact messenger pathway involved and whether the observed effects are affected by the presence of the $Ca_v2.1$ N terminus.

Novel Perspectives from Our Studies—Here we provide for the first time a functional description of an expressed invertebrate synaptic Ca_v2 calcium channel in a mammalian cell line.

First, we show here that properties of mammalian Ca_v2 channels cannot be universally applied to invertebrates, since toxin sensitivity and regulation of the channels by syntaxin1 appear to be unique to vertebrate channels. At the molecular level, such differences may in part reflect modifications or adaptations in the calcium-dependent neurotransmitter release process in either invertebrates or vertebrates.

Second, despite structural divergences, many of the characteristic biophysical features of mammalian P/Q- and N-type channels are found in the LCa_v2a-5′rbA channels. Selective permeability to ions (barium and calcium) and responsiveness to changes in membrane voltage, including the rate and threshold of activation and inactivation, are remarkably similar, suggesting that the fundamental biophysical characters responsible for calcium- and voltage-dependent synaptic transmission are conserved at the level of the calcium channel. This similarity is shared at a biophysical level of invertebrate synaptic transmission where kinetic features of calcium-dependent neurotransmitter release are comparable with mammalian ones.

Third, as we reported previously, the invertebrate channel LCa_v2a lacks an equivalent for the mammalian synaptic protein interaction (*synprint*) site in the II-III linker, enabling it to bind synaptic proteins such as *Lymnaea* syntaxin1 or even mammalian syntaxin1A. Conversely, there is a reverse compatibility from mammals to invertebrates, where mammalian *synprint* binds with high affinity to invertebrate synaptic proteins, including syntaxin1, SNAP-25, and synaptotagmin1 (21). A functional consequence is that application of a *synprint* peptide to an invertebrate synapse blocks synaptic transmission as has been reported in mammals (21). To our surprise however, the invertebrate syntaxin ($Lsytx_1$) does not appear to be functionally compatible with mammalian Ca_v2 channels. Even though $Lsytx_1$ is strikingly homologous to both mammalian syntaxin1A and syntaxin1B (see Fig. 7*C*) and capable of physically binding to $Ca_v2.2$ (21), we did not observe an $Lsytx_1$-induced reduction in $Ca_v2.2$ channel availability. This brings a unique perspective to the relationship between synaptic calcium channels and synaptic proteins, suggesting that Ca_v2 channels and syntaxin1 may have coevolved to allow for syntaxin-mediated regulation of Ca_v2 channel activity. Indeed, minor residue changes in syntaxin1 and more profound adaptations such as the insertion of a ~250–300-amino acid *synprint* domain into vertebrate Ca_v2 calcium channels appear required to allow a functional regulation of mammalian Ca_v2 channels by syntaxin1. The lack of this interaction in invertebrates may perhaps provide an opportunity to reconstitute functional interactions between synaptic calcium channels and synaptic proteins and investigate their consequences on synaptic release, thus providing novel insights into the intricacies of synaptic transmission.

Finally, identified synapses between *Lymnaea* neurons are highly amenable for analysis using molecular and electrophysiological approaches and optical imaging (21, 65–67). A combined approach using *in vitro* expression and hypothesis testing in native invertebrate neurons may, thus, permit us to dissect the interplay between presynaptic calcium channels, second messenger systems, and synaptic proteins.

Acknowledgments—We thank Dr. Terry Snutch for donating rat calcium channel subunits and Peter Larsen for technical assistance. We thank Dr. Wayne Giles for providing partial personnel support to L. Chen.

REFERENCES

1. Catterall, W. A. (2000) *Annu. Rev. Cell Dev. Biol.* **16,** 521–555
2. Atlas, D. (2001) *J. Neurochem.* **77,** 972–985
3. Wheeler, D. B., Randall, A., and Tsien, R. W. (1994) *Science.* **264,** 107–111
4. Birnbaumer, L., Qin, N., Olcese, R., Tareilus, E., Platano, D., Costantin, J., and Stefani, E. (1998) *J. Bioenerg. Biomembr.* **30,** 357–375
5. Felix, R. (1999) *Recept. Chan.* **6,** 351–362
6. Klugbauer, N., Dai, S., Specht, V., Lacinova, L., Marais, E., Bohn, G., and Hofmann, F. (2000) *FEBS Lett.* **470,** 189–197
7. Jarvis, S. E., and Zamponi, G. W. (2001) *Trends Pharmacol. Sci.* **22,** 519–525
8. Westenbroek, R. E., Hell, J. W., Warner, C., Dubel, S. J., Snutch, T. P., and Catterall, W. A. (1992) *Neuron* **9,** 1099–1115
9. Westenbroek, R. E., Hoskins, L., and Catterall, W. A. (1998) *J. Neurosci.* **18,** 6319–6330
10. Timmermann, D. B., Westenbroek, R. E., Schousboe, A., and Catterall, W. A. (2002) *J. Neurosci. Res.* **67,** 48–61
11. Wiser, O., Bennett, M. K., and Atlas, D. (1996) *EMBO J.* **15,** 4100–4110
12. Spafford, J. D., and Zamponi, G. W. (2003) *Curr. Opin. Neurobiol.*, in press
13. Currie, K. P., and Fox, A. P. (1997) *J. Neurosci.* **17,** 4570–4579
14. Zhang, J. F., Ellinor, P. T., Aldrich, R. W., and Tsien, R. W. (1996) *Neuron* **17,** 991–1003
15. De Waard, M., Liu, H., Walker, D., Scott, V. E., Gurnett, C. A., and Campbell, K. P. (1997) *Nature* **385,** 446–450
16. Kohn, A. B., Lea, J., Roberts-Misterly, J. M., Anderson, P. A., and Greenberg, R. M. (2001) *Parasitology* **123,** 489–497
17. Jeziorski, M. C., Greenberg, R. M., and Anderson, P. A. (2000) *J. Exp. Biol.* **203,** 841–856
18. Kawasaki, F., Felling, R., and Ordway, R. W. (2000) *J. Neurosci.* **20,** 4885–4889
19. Kawasaki, F., Collins, S. C., and Ordway, R. W. (2002) *J. Neurosci.* **15,** 5856–5864
20. Schafer, W. R., and Kenyon, C. J. (1995) *Nature* **375,** 73–78

21. Spafford, J. D., Munno, D. W., Van Nierop, P., Feng, Z. P., Jarvis, S. E., Gallin, W. J., Smit, A. B., Zamponi, G. W., and Syed, N. I. (2003) *J. Biol. Chem.* **278,** 4258–4267
22. Takahashi, T., and Momiyama, A. (1993) *Nature* **366,** 156–158
23. Kimura, T., and Kubo, T. (2002) *Neuroreport* **13,** 2389–2393
24. Kits, K. S., and Mansvelder, H. D. (1996) *Invert. Neurosci.* **2,** 9–34
25. Staras, K., Gyori, J., and Kemenes, G. (2002) *Eur. J. Neurosci.* **15,** 109–119
26. Jarvis, S. E., and Zamponi, G. W. (2001) *J. Neurosci.* **21,** 2939–2948
27. Ellinor, P. T., Zhang, J. F., Horne, W. A., and Tsien, R. W. (1994) *Nature* **372,** 272–275
28. Bezprozvanny, I., Scheller, R. H., and Tsien, R. W. (1995) *Nature* **378,** 623–626
29. Degtiar, V. E., Scheller, R. H., and Tsien, R. W. (2000) *J. Neurosci.* **20,** 4355–4367
30. Kaneko, S., Cooper, C. B., Nishioka, N., Yamasaki, H., Suzuki, A., Jarvis, S. E., Akaike, A., Satoh, M., and Zamponi, G. W. (2002) *J. Neurosci.* **22,** 82–92
31. Roullet, J. B., Spaetgens, R. L., Burlingame, T., Feng, Z. P., and Zamponi, G. W. (1999) *J. Biol. Chem.* **274,** 25439–25446
32. Jarvis, S. E., Barr, W., Feng, Z. P., Hamid, J., and Zamponi, G. W. (2002) *J. Biol. Chem.* **277,** 44399–44407
33. Bourinet, E., Zamponi, G. W., Stea, A., Soong, T. W., Lewis, B. A., Jones, L. P., Yue, D. T., and Snutch, T. P. (1996) *J. Neurosci.* **16,** 4983–4993
34. Zamponi, G. W., and Snutch, T. P. (1996) *Pfluegers Arch. Eur. J. Physiol.* **431,** 470–472
35. Kumar, P. P., Stotz, S. C., Paramashivappa, R., Beedle, A. M., Zamponi, G. W., and Rao, A. S. (2002) *Mol. Pharmacol.* **61,** 649–658
36. Feng, Z. P., Hamid, J., Doering, C., Bosey, G. M., Snutch, T. P., and Zamponi, G. W. (2001) *J. Biol. Chem.* **276,** 15728–15735
37. Sather, W. A., and McCleskey, E. W. (2003) *Annu. Rev. Physiol.* **65,** 133–159
38. Yang, J., Ellinor, P. T., Sather, W. A., Zhang, J. F., and Tsien, R W. (1993) *Nature* **366,** 158–161
39. Arnot, M. I., Stotz, S. C., Jarvis, S. E., and Zamponi, G. W. (2000) *J. Physiol.* **527,** 203–212
40. Zamponi, G. W., Bourinet, E., Nelson, D., Nargeot, J., and Snutch, T. P. (1997) *Nature* **385,** 442–446
41. Bourinet, E., Soong, T. W., Stea, A., and Snutch, T. P. (1996) *Proc. Natl. Acad. Sci. U. S. A.* **93,** 1486–1491
42. Zamponi, G. W., and Snutch, T. P. (1998) *Curr. Opin. Neurobiol.* **8,** 351–356
43. Zamponi, G. W., and Snutch, T. P. (1998) *Proc. Natl. Acad. Sci. U. S. A.* **95,** 4035–4039
44. Barrett, C. F., and Rittenhouse, A. R. (2000) *J. Gen. Physiol.* **115,** 277–286
45. Man-Son-Hing, H., Zoran, M. J., Lukowiak, K., and Haydon, P. G. (1989) *Nature* **341,** 237–239
46. Man-Son-Hing, H., and Haydon, P. G. (1992) *Neurosci. Lett.* **137,** 133–136
47. Yakel, J. L. (1991) *J. Neurophysiol.* **65,** 1517–1527
48. Brezina, V., Eckert, R., and Erxleben, C. (1987) *J. Physiol.* **388,** 565–595
49. Dreijer, A. M. Verheule, S., and Kits, K. S. (1995) *Invert. Neurosci.* **1,** 75–86
50. Jarvis, S. E., Magga, J. M., Beedle, A. M., Braun, J. E., and Zamponi, G. W. (2000) *J. Biol. Chem.* **275,** 6388–6394
51. Stotz, S. C., Hamid, J., Spaetgens, R. L., Jarvis, S. E., and Zamponi, G. W. (2000) *J. Biol. Chem.* **275,** 24575–24582
52. Stotz, S. C., and Zamponi, G. W. (2001) *J. Biol. Chem.* **276,** 33001–33010
53. Stotz, S. C., and Zamponi, G. W. (2001) *Trends Neurosci.* **24,** 176–181
54. Herlitze, S., Hockerman, G. H., Scheuer, T., and Catterall, W. A. (1997) *Proc. Natl. Acad. Sci. U. S. A.* **94,** 1512–1516
55. Berjukow, S., Marksteiner, R., Sokolov, S., Weiss, R. G., Margreiter, E., and Hering, S. (2001) *J. Biol. Chem.* **276,** 17076–17082
56. Hering, S., Berjukow, S., Sokolov, S., Marksteiner, R., Weiss, R. G., Kraus, R., and Timin, E. N. (2000) *J. Physiol.* **528,** 237–249
57. Budde, T., Meuth, S., and Pape, H. C. (2002) *Nat. Rev. Neurosci.* **3,** 873–883
58. Zuhlke, R. D., Pitt, G. S., Deisseroth, K., Tsien, R. W., and Reuter, H. (1999) *Nature* **399,** 159–162
59. Peterson, B. Z., DeMaria, C. D., Adelman, J. P., and Yue, D. T. (1999) *Neuron* **22,** 549–558
60. Lee, A., Wong, S. T., Gallagher, D., Li, B., Storm, D. R., Scheuer, T., and Catterall, W. A. (1999) *Nature* **399,** 155–159
61. Wappl, E., Mitterdorfer, J., Glossmann, H., and Striessnig, J. (2001) *J. Biol. Chem.* **276,** 12730–12735
62. Huber, I., Wappl, E., Herzog, A., Mitterdorfer, J., Glossmann, H., Langer, T., and Striessnig, J. (2000) *Biochem. J.* **347,** 829–836
63. Qin, N., Platano, D., Olcese, R., Stefani, E., and Birnbaumer, L. (1997) *Proc. Natl. Acad. Sci. U. S. A.* **94,** 8866–8871
64. Canti, C., Page, K. M., Stephens, G. J., and Dolphin, A. C. (1999) *J. Neurosci.* **19,** 6855–6864
65. Smit, A. B., Syed, N. I., Schaap, D., van Minnen, J., Klumperman, J., Kits, K. S., Lodder, H., van der Schors, R. C., van Elk, R., Sorgedrager, B., Brejc, K., Sixma, T. K., and Geraerts, W. P. (2001) *Nature* **411,** 261–268
66. Feng, Z. P., Grigoriev, N., Munno, D., Lukowiak, K., MacVicar, B. A., Goldberg, J. I., and Syed, N. I. (2002) *J. Physiol.* **539,** 53–65
67. van Kesteren, R. E., Syed, N. I., Munno, D. W., Bouwman, J., Feng, Z. P., Geraerts, W. P., and Smit, A. B. (2001) *J. Neurosci.* **21,** RC161